MODELING OF BRICK MASONRY INFILL AND APPLICATION TO ANALYSES OF INDONESIAN R/C FRAME BUILDINGS

Maidiawati[1*†], and Y. SANADA[2]

[1] *Graduate School of Engineering, Toyohashi University of Technology, Japan*
[2]*Associate Professor, Osaka University, Japan*

ABSTRACT

This paper presents a simple strut model to evaluate the seismic performance of reinforced concrete frame structures considering the brick masonry infill effects. In this model, the equivalent strut width is presented as a function of infill/frame contact length which can be determined by solving two equations considering the compression balance at infill/frame interface and lateral displacement compatibility.

An experimental verification using bare frame and brick masonry infilled frame was conducted. Good agreements were observed between the experiment and analytical simulation on lateral stiffness, lateral strength, and ductility. The analytical model was applied to nonstructural brick infill in two Indonesian earthquake-damaged buildings. It was found nonstructural brick infill significantly contributed to the seismic resistances of damaged buildings.

Keywords: Infill/frame contact length, nonstructural wall, reinforced concrete frame, seismic performance, strut width.

1. INTRODUCTION

Brick masonry walls are commonly used as infill in Indonesian R/C buildings. However, the presence of brick masonry infill in such buildings is usually neglected in seismic design calculations, assuming it to be a nonstructural element. According to experimental and analytical past studies, the brick masonry infill significantly contributed to the seismic performance of this kind of buildings (Maidiawati et al. 2011). A number of researchers have studied analytical models for evaluating contribution of infill to frame structures based on diagonal struts caused in masonry infill, as reported in several references (El-Dakhakhni et al. 2003; Paulay and Priestley 1992; Stafford and Carter 1969).

This study proposes an alternative method for modeling the brick masonry infilled frames with simplified equations. In this model, the equivalent strut width is presented as a function of infill/frame contact length which can be determined by solving two equations, i.e., static

* Corresponding author: Email: maidiawati@yahoo.com

† Presenter: Email: maidiawati@yahoo.com

equilibriums related to the compression balance at infill/frame interface and lateral displacement compatibility.

A series of reversed cyclic lateral loading tests on bare frame and brick masonry infilled frame structures was conducted to verify the proposed analytical model. Experimental specimens represented an Indonesian earthquake-damaged building investigated by the authors after the 2007 Sumatra earthquakes (Maidiawati and Sanada 2008). Seismic performance evaluations were also performed on two R/C buildings: collapsed and surviving buildings, by applying the analytical model to nonstructural brick infill.

2. MODELLING OF MASONRY INFILLED FRAMES

This study targets brick masonry infilled R/C frames with relatively stiff beams which are typically used in Indonesian buildings, as shown in Figure 1(a). Such infilled frames may also represent the lower part of multi-story confined masonry structures where beam flexural deformation is constrained by the existence of infill. When they deform under lateral loads, contact/separation is caused between the bounding column and infill due to column flexural deformation and infill shear deformation, as shown in Figure 1(b). In this study, the contact length was derived from a simple procedure for the seismic performance evaluation of the targeted structures.

(a) RC building with brick masonry infill

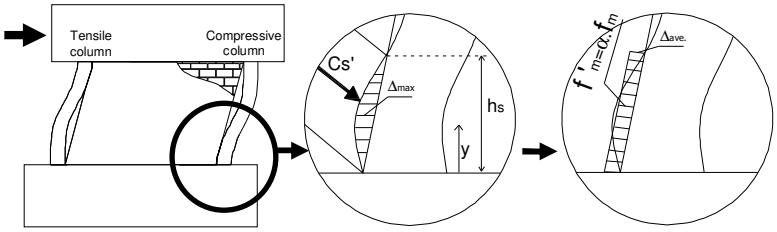

(b) Interface of infill/frame under lateral deformation of infilled frame

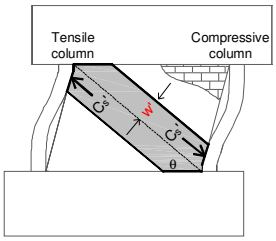

(c) Diagonal compression at infill/column interface

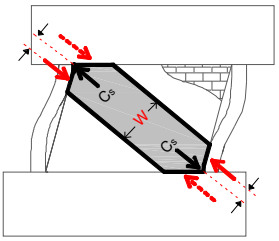

(d) Derivation of strut width

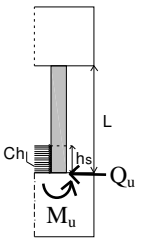

(e) Distributed strut force

Figure 1: Modeling of masonry-infilled frame.

The masonry infill panel was replaced by a diagonal compression strut having the same thickness and material properties as those of the panel. In this model, a compression stress distribution at the infill/frame interface was replaced by an equivalent rectangular block, as shown in Figure 1(b), where the averaged compressive strength, f_m', was evaluated by multiplying the uniaxial compressive strength of infill, f_m, by a reduction factor, α, which was evaluated by Equation (1).

The diagonal compression, C_s', which acts on the bottom/top of the compressive/tensile column as shown in Figure 1(c), is given by Equation (2a). However, assuming reaction forces at the column ends, an unbalanced moment causes a rotation of a free body of the infill, as shown by the solid red arrows in Figure 1(d). Therefore, reaction forces were considered at the beam ends, as shown by the dashed arrows in the figure. As a result, the total diagonal compression, C_s, was represented by twice as C_s', as given by Equation (2b). Then, C_s was resolved into the horizontal and vertical components, which were represented by the distributed forces along column height, as shown in Equations (2c) and (2d).

$$\alpha = \frac{\Delta_{ave}}{\Delta_{\max}} = \frac{\int_0^{hs} \Delta(y)dy / hs}{\Delta_{\max}} \tag{1}$$

$$C_s' = 1/2\, w' t f_m' \tag{2a}$$

$$C_s = W t f_m' \tag{2b}$$

$$c_h = t f_m' \cos^2\theta \tag{2c}$$

$$c_v = t f_m' \sin\theta \cos\theta \tag{2d}$$

in which, α: reduction factor, $\Delta(y)$: difference between flexural ($\delta_f(y)$) and shear ($\delta_s(y)$) deformation along column height, so $\Delta(y)=\delta_s(y)-\delta_f(y)$, Δ_{ave}: averaged difference between flexural and shear deformation, Δ_{max}: maximum difference between flexural and shear deformation, w': half strut width from diagonal axis, t: thickness of infill, W: strut width, $W=2w'$, θ: inclination angle of strut, as shown in Figure 1(c).

Assuming that the compressive column yields in flexure at the bottom, the moment distribution along column height, ${}_cM(y)$, is obtained with Equation (3). Yield moment, however, is calculated with Equation (4) based on the Japanese standard (JBDPA 2005).

In the case of $0 \le y \le h_s$

$${}_cM(y) = {}_{y=0}M_u - Q_u y + 1/2 C_h y^2 \tag{3a}$$

In the case of $h_s \le y \le L$

$${}_cM(y) = {}_{y=0}M_u - Q_u y + C_h h_s y - 1/2 C_h h_s^2 \tag{3b}$$

$$M_u = 0.8 a_t \sigma_y D + 0.5 N D\left(1 - \frac{N}{b D F_c}\right) \tag{4}$$

where, h_s: infill/column contact height, as shown in Figure 1(b), L: clear column height, as shown in Figure 1(e), M_u: flexural strength of column, Q_u: shear force at column bottom, which is determined with Equation (6), as derived later, a_t: total cross-sectional area of tensile reinforcing bars, σ_y: yield stress of longitudinal reinforcement, D: column depth, N: axial force, b: column width, F_c: compressive strength of concrete. However, the axial force at the bottom of column was calculated as a summation of building weight (initial axial load), N_a, axial force due to shearing force in the beam, N_b, and vertical component of the strut force, $C_v h_s$, as shown in Figure 2.

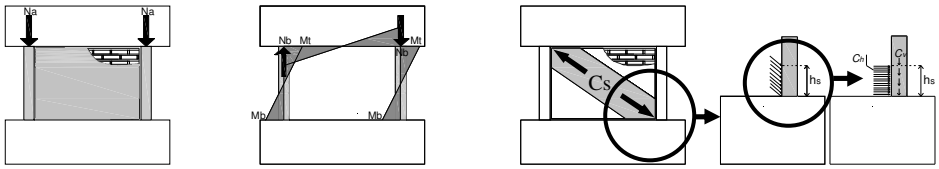

(a) Initial axial load b) Axial load due to shear force in beam (c) Axial force due to strut force

Figure 2: Consideration of axial force at column bottom.

Lateral displacement along column height, ${}_c\delta(y)$, is produced by double integrals of Equation (3)/*EI*, which is shown by Equation (5).

In the case of $0 \le y \le h_s$

$$ {}_c\delta(y) = \frac{1}{EI}\left(1/24\, C_h y^4 - 1/6\, Q_u y^3 + 1/2\, M_u y^2\right) \tag{5a} $$

In the case of $h_s \le y \le$ L

$$ {}_c\delta(y) = \frac{1}{EI}\left(\left(1/6 C_h h_s - 1/6 Q_u\right) y^3 + \left(1/2 M_u - 1/4 C_h h_s^2\right) y^2 + 1/6\, C_h h_s^3\, y - 1/24\, C_h h_s^4\right) \tag{5b} $$

where, *E* and *I* are Young's modulus and the second moment of inertia of columns. Shear force at the bottom of compressive column, Q_u is given by Equation (6) when assuming a rotation of zero at the column top.

$$ Q_u = \frac{2M_u}{L} + C_h h_s - \frac{C_h h_s^2}{L} + \frac{C_h h_s^3}{3L^2} \tag{6} $$

On the other hand, lateral deformation along infill height, ${}_i\delta(y)$, is defined by Equation (7), assuming a uniform shear strain, ${}_i\theta$. Therefore, intersection height between column and infill can be evaluated by solving Equation (8), as shown in Figure 3. Therefore, unknown h_s is obtained through an iteration after satisfying $y = h_s$.

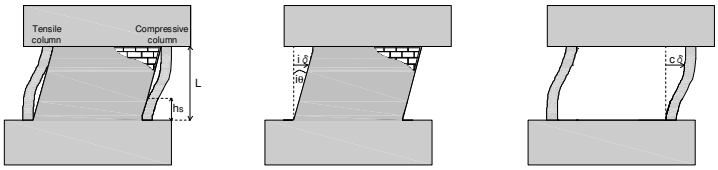

(a) Infilled frame (b) Infill (c) RC frame

Figure 3: Lateral displacement compatibility between column and infill.

$$ {}_i\delta(y) = {}_i\theta\, y = \frac{{}_c\delta(y = L)}{L} y \tag{7} $$

$$ {}_c\delta(y) = {}_i\delta(y) = \frac{{}_c\delta(y = L)}{L} y \tag{8} $$

Consequently, the width of compression strut, *W*, is determined as a function of infill/column contact height, by Equation (9), however, which is defined as the smallest contact lengths between both ends of the strut.

$$W = 2h_s \cos\theta \tag{9}$$

3. EXPERIMENTS FOR VERIFICATION

The proposed method was verified through the authors' past experiments of R/C bare frame (BF) and brick infilled frame (IF) specimens (Maidiawati et al. 2011). Based on the test results, Figure 4 shows the relationships between lateral force and drift ratio for both specimens. The infill contribution was extracted by evaluating the difference between lateral forces of IF and BF specimens at each load step (at the same drift ratio), as shown in Figure 5.

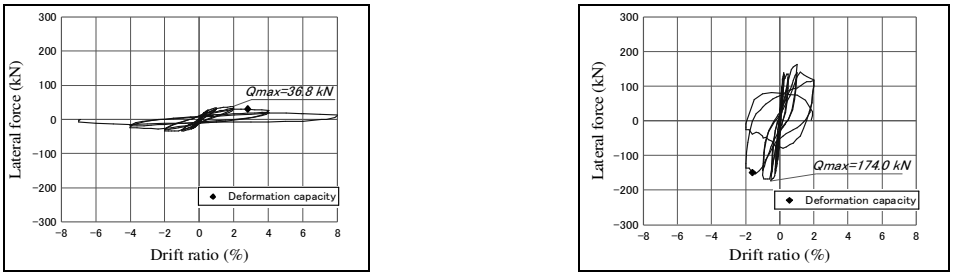

(a) BF specimen (b) IF specimen

Figure 4: Lateral force–drift ratio relationships.

4. VERICATION OF ANALYTICAL MODEL

The envelope curve of infill was simulated by a trilinear model, in which the cracking force, V_c, and displacement, δ_c, of infill were defined by Equations (10) and (11), respectively, assuming that the infill/column independently behaved at a small drift considering the imperfect connection between both.

$$V_c = \tau A_w \tag{10}$$

$$\delta_c = \frac{\nu' V_c h}{G A_w} \tag{11}$$

$$G = \frac{E_m}{2(1+\nu)} \tag{12}$$

where, τ: shear strength of infill obtained by $\tau=f_t$, in which f_t is tensile strength of brick unit as the weakest component of infill, A_w: cross-section area of infill, ν': shear deformation coefficient which is equal to 1.2 for a rectangular cross-section, h: height of infill, G: shear modulus of infill obtained by Equation (12), E_m: elastic modulus of masonry infill, ν: poison ratio of masonry wall.

According to the proposed analytical method, the infill/column contact length of IF specimen, h_s, was evaluated to be 270 mm, hence the strut width was obtained by Equation (9). Equations (13) and (14) give the lateral strength, V_m, and secant stiffness, K, at a yielding of strut, respectively.

$$V_m = W t f_m' \cos\theta \tag{13}$$

$$K = \frac{E_m W t}{d_m} \cos^2\theta \tag{14}$$

where, d_m: diagonal length of infill.

The performance curve evaluated as above is compared to the envelope of the experimental result in Figure 5. A good agreement was obtained between both, which verified that the proposed method could be used for estimating the seismic performance of masonry infill.

Moreover, the performance of compressive column was also replaced by a bilinear model, as shown in Figure 6. In the figure, however, the column shear was represented by the average of shear force, ${}_cQ(y)$ which is the first differential of Equation (3), along the column height equal to column depth (y=D) from the end, because the severe damage occurred across this section. The drift at the maximum shear, D_{Ry}, should be given by Equation (15) considering the lateral displacement compatibility. On the other hand, the shear capacity of column was evaluated by Equation (16) (Priestley et al. 1994), where the parameters of P and a were evaluated considering the strut effects. The deformation capacity of column was defined as a drift where shear force attained to the capacity, as shown in Figure 6. Consequently, it was 0.016 rad. which agreed with the experiment.

$$D_{Ry} = V_m / (K.L) \tag{15}$$

$$V_n = k\sqrt{F_c}(0.8A_g) + \frac{A_v f_y D'}{s}\cot 30^o + \frac{D-c}{2a}P \tag{16}$$

where, k: degradation of concrete strength which is 0.29 MPa up to a drift of 0.01 and 0.1 MPa at a drift of 0.02, as shown in Figure 6, A_g: gross cross-sectional area of column, A_v: cross-sectional area of hoop, f_y: yield stress of hoops, D': distance between the centers of hoop, s: spacing between hoops along the axis, c: neutral axis depth, P: axial force, a: shear span.

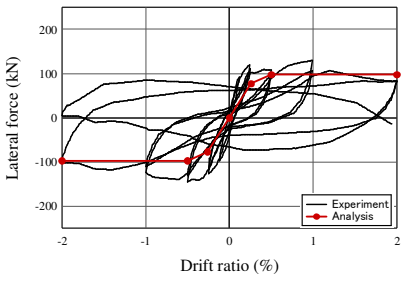

Figure 5: Lateral force-drift ratio relationship of brick infill.

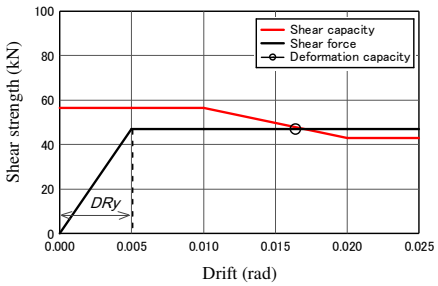

Figure 6: Performance curve of column with infill effects.

5. SEISMIC PERFORMANCE EVALUATION OF R/C BUILDINGS

The proposed model was applied to nonstructural brick infill in the collapsed and moderately damaged buildings due to the 2007 Sumatra earthquakes (Maidiawati and Sanada 2008). The surviving building was structurally similar to the collapsed one, as shown in Figure 7. The material properties of buildings were 26.7 N/mm^2, 307 N/mm^2 and 240 N/mm^2 for concrete compression strength, yield strength of longitudinal and transverse reinforcements, respectively.

Seismic performance of both buildings was evaluated only for the first story on the basis of the

Japanese standard (JBDPA 2005). The proposed analytical model was applied to evaluate the infill effects. In the case of multi-span infilled frames, however, each column was categorized into an exterior tensile column, interior column and exterior compressive column, as shown in Figures 8(a), (b) and (c), respectively. In particular, distributed forces due to the struts were antisymmetrically applied to the bottom and top of interior column, as shown in Figure 8(b). Consequently, shear force at the interior column end was determined by Equation (17).

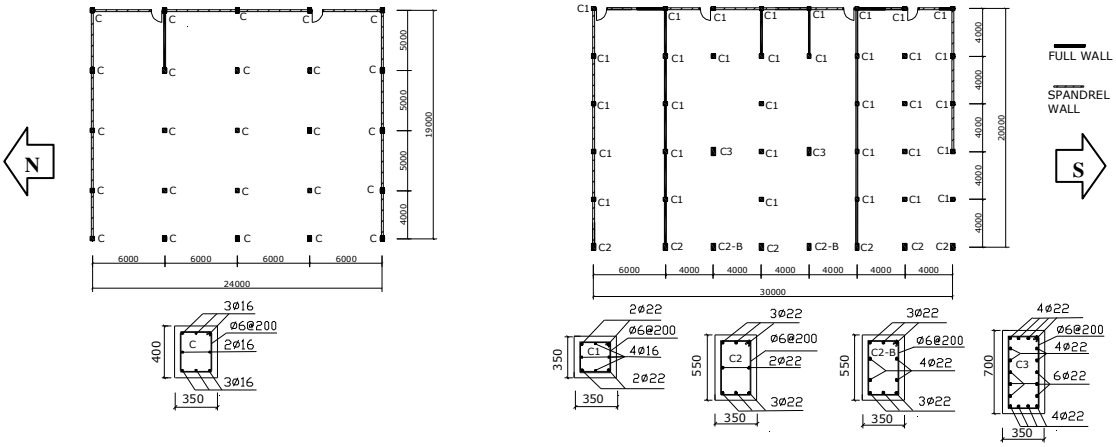

(a) Collapsed building (b) Surviving building

Figure 7: First floor plan and column details of damage buildings.

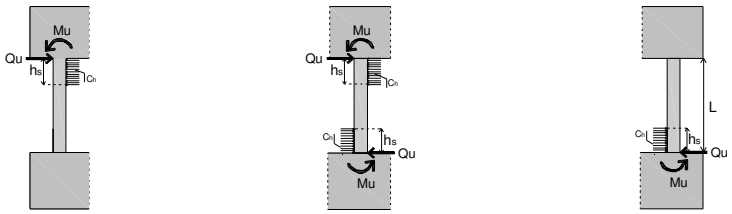

(a) Exterior tensile column (b) Interior column (c) Exterior comoressive column

Figure 8: Assumed distributed forces due to struts at column ends.

$$Q_u = \frac{2M_u}{L} + C_h h_s - \frac{C_h h_s^{\,2}}{L} \tag{17}$$

The seismic performance of buildings was represented as a *C-F* relationship based on the reference of JBDPA. The cumulative strength index, *C*, at a certain ductility index, *F*, was calculated by Equation (18).

$$C = C_i + \sum \alpha_j C_j \tag{18}$$

$$C_i = \frac{Q_{ui}}{\sum W} \tag{19}$$

where, C_i: strength index of the *i*-th group of vertical members having the same ductility index, given by Equation (19), α_j: effective strength factor of the *j*-th group for considering differences between yield deformations of *i*- and *j*-th groups, C_j: strength index of the *j*-th group having the same ductility index larger than that of *i*-th group, Q_{ui}: ultimate lateral load-carrying capacity of the i-th group of vertical members, ΣW: total weight of building supported by the story concerned.

The ductility index, *F* represents deformability of certain vertical members calculated according to structural specifications based on the reference. In the case of columns with infill effects, deformation capacities of the columns were evaluated in the same manner as mentioned in the previous section.

Calculated seismic performance of both buildings is compared in the E-W direction, as shown in Figure 9. The strength of collapsed building drastically dropped at a 1.0% drift, as shown in Figure 9(a). On the other hand, the strength of surviving building was maintained until more than 2.0% drift, as shown in Figure 9(b). This is a possible reason why one of the buildings could survive during the severe earthquake ground motions.

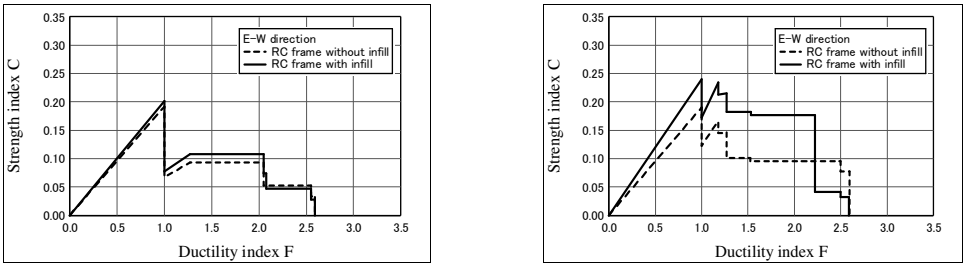

(a) Collapsed building (b) Surviving building

Figure 9: Seismic performance of the collapsed and surviving buildings.

6. CONCLUSIONS

A new analytical model was proposed to evaluate the contribution of brick masonry infill in R/C frames and verified through the authors' past experiments. As the results, a good agreement was observed between the experimental and analytical results. The proposed method was implemented for the seismic performance evaluation of two earthquake-damaged Indonesian buildings. It was found that brick masonry infill significantly contributed to the seismic resistances and prevented a total collapse of the surviving building.

REFERENCES

El-Dakhakhni WW, Elgaaly M, and Hamid AA (2003). Three-Strut model for concrete masonry-infilled steel frames. Journal of Structural Engineering. 129 (2), pp. 107-185.

Maidiawati and Sanada Y (2008). Investigation and analysis of buildings damaged during the September 2007 Sumatra, Indonesia earthquakes. Journal of Asian Architecture and Building Engineering. 7(2), pp. 371–378.

Maidiawati, Sanada Y, Konishi D, and Tanjung J (2011). Seismic performance of nonstructural brick walls used in Indonesian R/C buildings. Journal of Asian Architecture and Building Engineering. 10 (1), pp. 203-210.

Paulay T, and Priestley MJN (1992). Seismic design of reinforced concrete and masonry buildings. John Wiley & Sons, Inc.

Priestley MJN, Verma R and Xiao Y (1994). Seismic shear strength of reinforced concrete columns. Journal of Structural Engineering. 120(8), pp.2310-2329.

Stafford Smith B and Carter C (1969). A method of analysis for infilled frames. Proc. ICE. 44, pp. 31-48.

The Japan Building Disaster Prevention Association (JBDPA) (2005). English version, 1st, Standard for seismic evaluation of existing reinforced concrete buildings, 2001.